Earth Planet. Sci. Lett. 628 (2024) 118583

Contents lists available at ScienceDirect

Earth and Planetary Science Letters

journal homepage: www.elsevier.com/locate/epsl

Autogenic masking of allogenic inputs: Numerical modelling of signal preservation in deep-water fan strata

Peter M. Burgess *, Robert A. Duller

Jane Herdman Laboratory, Department of Earth, Oceans and Ecological Science, University of Liverpool, Liverpool L69 3GP, United Kingdom

ARTICLE INFO

Editor: J.P. Avouac

Keywords:
Sequence stratigraphy
Source-to-sink
Allogenic
Autogenic
Deep-water fan
Stratigraphic forward modelling

ABSTRACT

Variations in climate, sea-level and tectonic processes can be recorded in various ways in strata, and recognising and measuring such external signals preserved in strata is an important aspect of deciphering Earth history. Key questions are what type of signals are likely to be preserved; how input signals may be shredded, over-printed or otherwise reduced before preservation, by stochastic or autogenic processes; and how allocyclic products may be mimicked and masked by autogenic processes. A reduced-complexity numerical forward model of down-slope sediment erosion, transport and dispersive deposition of submarine fan strata is the simplest-possible formulation that produces reasonably realistic strata that can be robustly analysed for signal content across model realisations with a range of external forcing amplitudes and periods. Three different initial topographic surfaces that include increasing influence of random noise allow comparison of the signal preserved with different levels of random influence on the deterministic model. Spectral analysis, with rigorous testing for statistical significance, shows that the signal recorded depends strongly on the level of noise present in the underlying topography, that short-period high-amplitude allocyclic signals are the most likely to be preserved in this case, and that autogenic dynamics in the modelled system can effectively mask even long-period high-amplitude input signals because they have similar periodicities. Autogenic processes in this model can also produce 5:1 bundling of cyclical strata commonly assumed to be strong evidence for orbital forcing. This analysis suggests that we might be substantially underestimating the complexity involved in extracting a signal of external forcing from strata where any autogenic processes operate, to the extent that the two different effects may often be practically indistinguishable, indicating that a multiple hypothesis approach is important to account for the resulting uncertainty.

1. Introduction

Strata are often analysed to identify what, if any, signal they contain that records climate change, sea-level variations, or tectonic events (e.g. Blum et al., 2018; Somme et al., 2019; Straub et al., 2019; Tofelde et al., 2021; Sharman et al., 2023). Such analysis is an important element in reconstructing Earth history, but preservation and subsequent identification of external signals in strata is complicated. Analysis of the fundamental processes of sediment transport through source-to-sink systems (Paola et al., 1992; McNab et al., 2023) demonstrate how variations in climate and tectonic processes can be recorded as an input signal, but also how the complexity of sediment transport systems can entirely destroy, or shred, that input signal (Jerolmak and Paola, 2010). Analyses tend to distinguish zones of signal generation in erosional areas from signal modification through transfer zones, to signal preservation in areas of deposition (e.g. Allen, 2017), but the complexity of such systems means that zones of erosion that generate a recordable signal can occur all along a source-to-sink system, from mountain slopes to basin-margin clinoform slopes.

Reliable reconstructions of input signals therefore require a full understanding of this complexity in preservation and identification (Tofelde et al., 2021). A key issue is the question of how autogenic process can mask, disrupt, or erase an external signal (Burgess, 2006; Hajek and Straub, 2017; Toby et al., 2019; Griffin et al., 2023). Related to this, uncertainty remains what type of external signal is most likely to be preserved, with documented examples of signal-generating processes and preserved signals over a range of periods (Jobe et al., 2015; Bernhardt et al., 2017; Vandekerkhove et al., 2020; Tofelde et al., 2021) but an emphasis in many studies on preservation of relatively longer-period signals (e.g. Toby et al., 2019; Griffin et al., 2023). Another issue is how

* Corresponding author.
E-mail address: pmb42@liverpool.ac.uk (P.M. Burgess).

https://doi.org/10.1016/j.epsl.2024.118583
Received 10 July 2023; Received in revised form 23 December 2023; Accepted 13 January 2024

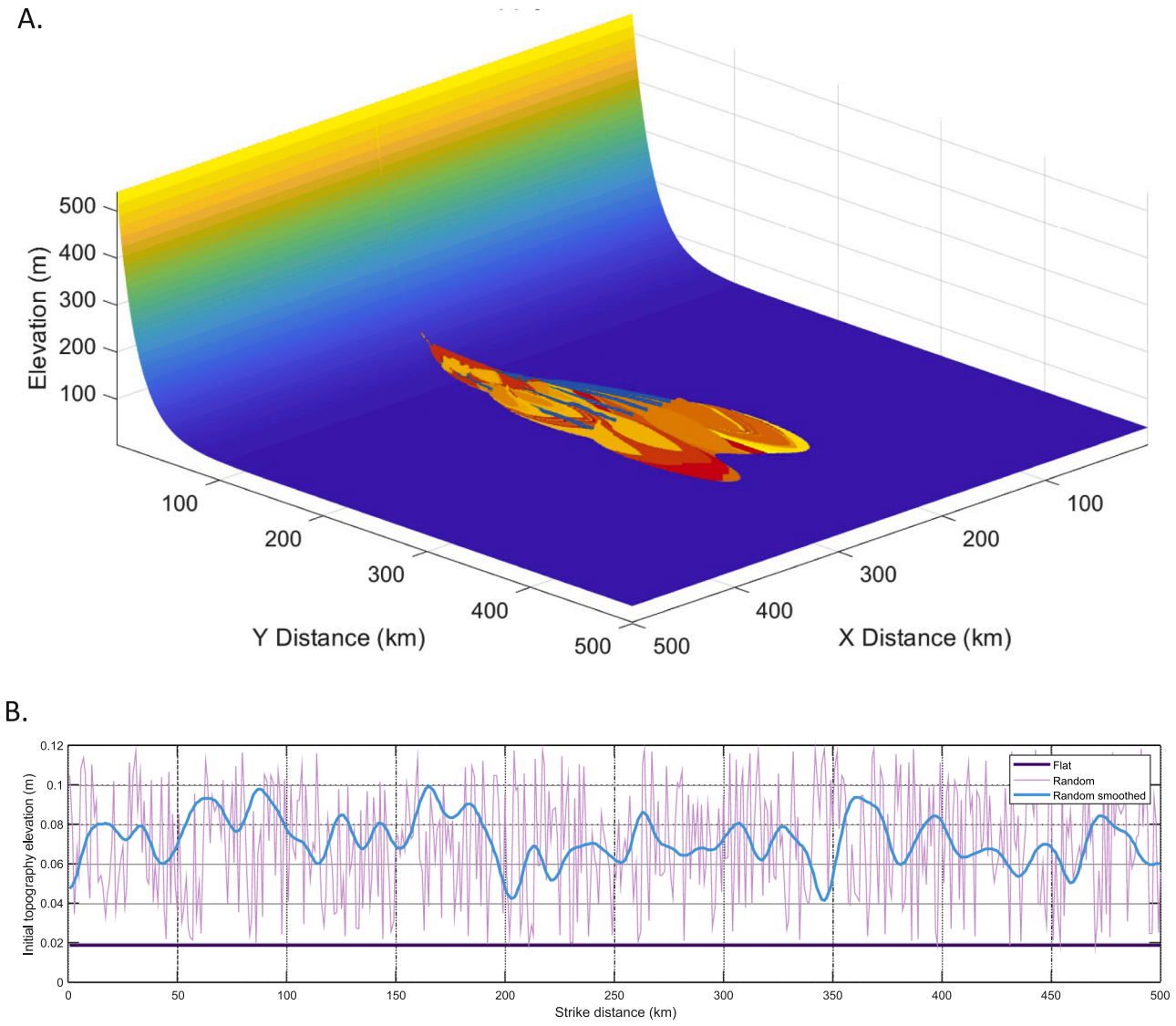

Fig. 1. A. The slope-to-basin-floor concave-upwards topography used in all the models, showing channel routes (blue lines) and deposited strata from flows (red-to-yellow patches) from the constant supply no-noise model run. B Strike cross sections at $y = 200$ km showing the elevation of the no noise, smoothed noise, and raw random noise topographies used in the three model sets.

to analyse strata without making excessive *a priori* assumptions about the signal likely to be preserved, typically that the signal is external, not autogenic. For example, in many studies conclusions that strata are orbitally forced may mostly reflect the starting assumptions of the study (e.g. Abels et al., 2013; Scotchman et al., 2015; Qi et al., 2022).

Modelling studies are particularly useful for robust analysis of these questions because they tend to allow better isolation of cause-and-effect relationships through careful experimental design that is usually not possible studying outcrop or subsurface data directly (Burgess, 2012). Analogue experiments have the significant advantage of real physics, albeit with the important caveat of scaling issues, and flume tank experiments in various forms have played a large role thus far in generating some good understanding of how signal preservation works especially in fluvial and deltaic systems (e.g. Sheets et al., 2002; Paola et al., 2009; Foreman and Straub, 2017; Toby et al., 2019) but also in deep-marine systems (Ferguson et al., 2020; Spychala et al., 2020). Numerical modelling studies are also making an increasingly important contribution (e.g. Granjeon et al., 2014; Harris et al., 2016; Zhang et al. 2019, Wahab et al., 2022).

Reduced complexity numerical models may be particularly useful in this area, for three key reasons. Firstly, because they are fast to compute, it is possible to run many models, as often required for robust analysis. Secondly, because they are relatively simple and can be fully interrogated to any required level of detail, it is usually possible to extract simple but useful cause-and-effect explanations from the model output (Burgess, 2012). Finally, and most importantly, reduced-complexity models typically represent the simplest possible formulation that can produce and explain specific processes and products, and this simplicity offers potential to develop fundamental understanding of those processes and products.

The aim of this study is to use Lobyte3D, a reduced-complexity event-based numerical stratigraphic forward model of deep-water fan deposition (Burgess et al., 2019; Mackie et al., in review), to explore how allogenic forcing with a range of period and amplitudes is recorded in strata deposited in a system that also includes significant autogenic processes and a component of random noise, both of which may disrupt, mask or even shred the input signal. Unlike many other numerical forward models of turbidite systems, Lobyte3D is particularly useful because it models strata on a flow-by-flow and therefore bed-by-bed scale and can reproduce basic aspects of observed deep-water fan lobate geometries (Chen et al., 2023), allowing analysis of the model output at a scale and resolution similar to and therefore comparable

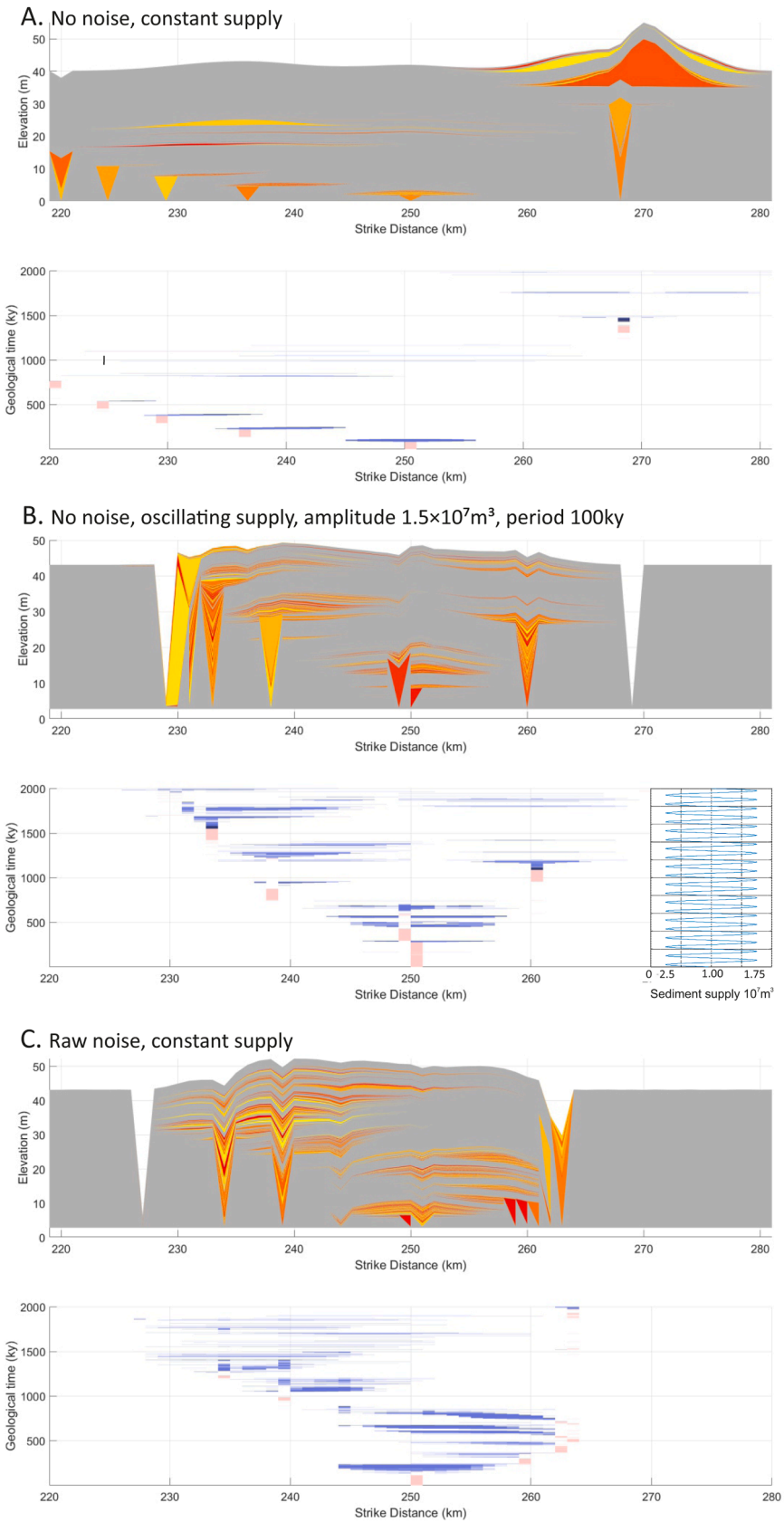

(caption on next page)

Fig. 2. A. Strike-oriented cross sections (individual flow deposits coloured red-to-yellow, background hemipelagic strata grey) and equivalent chronostratigraphic diagram (channel fill strata pink, lobe strata blue, thicker lines represent time-contiguous deposition) at $y = 155$ km from the constant supply case in the no-noise initial topography model set. Note how for the first 700ky of elapsed model time the channels and lobes migrate consistently leftwards from $x = 250$ km to $x = 220$ km because of the flat basin floor topography and bias in flow direction selection (see text), and then generally rightwards to $x = 270$ km, but with more variation due to the influence of developing depositional topography. B. Strike oriented cross-section and chronostratigraphic diagram from a model run in model Set 1 with no-noise initial topography and oscillating sediment supply (amplitude $1.5 \times 10^7 m^3$, period 100ky). Note how the variation in sediment supply disrupts the simple lobe migration pattern, shown in A, to produce more variable, complex stacking, channel cutting and channel fill episodes. C. Strike oriented cross-section and chronostratigraphic diagram from a model run in model Set 3 with raw random noise in the initial topography and constant sediment supply. In this case the substantially more variable stacking shown is due to the influence of the random noise in the initial topography which although low-relief (up to 0.1 m) is enough to disrupt the simple stacking patterns seen in A.

with outcrop, core and well-log. It is also particularly useful because it has a very simple numerical model formulation that allows full analysis and understanding of the model behaviour, and keeping the model formulation and parameters as simple as possible should provide a useful baseline to better understand the origins of more complex stacking patterns and recorded signals measured in outcrop and subsurface strata.

2. Method

2.1. Lobyte3D model formulation

Lobyte3D version 2.0 is reduced complexity numerical forward model of turbidite deposition described in Burgess et al. (2019). Version 2.0 has been enhanced to include erosion flow acceleration and deceleration, and simple flow-stripping leading to deposition of some flow volume behind topographic barriers, all as described in Chen et al. (2023). Down-slope sediment transport and erosion are modelled with all the sediment in a single 1 km by 1 km model cell following a steepest-descent algorithm. Erosion produces channels, particularly during intervals of flow re-routing and avulsion. Flow velocity is a function of downslope gravitational driving force, and if velocity exceeds a calculated threshold, the flow erodes and entrains sediment following Halsey (2018). When the gradient drops below a defined threshold of deposition, the flow disperses from each cell it flows into to all unoccupied adjacent cells with elevation lower than the current cell. Deposition occurs as a simple specified proportion of the flow volume present in each cell.

2.2. Model sets and the hypotheses they test

The analysis comprises three sets of model runs. Each model set comprises 28 model runs with similar concave slope-to-basin-floor initial topography (Fig. 1A). Model Set 1 uses this no-noise initial topography (Fig. 1B), Model Set 2 has added smoothed random noise with a pre-smoothing maximum amplitude of 0.1 m (Fig. 1B), and Model Set 3 has raw uncorrelated random noise with a maximum amplitude of 0.1 m added to the initial topography (Fig. 1B). Although low-amplitude, because the model formulation is sensitive to basin-floor topography, even 10 cm height difference across grid points is enough to affect flow routing on the otherwise low-gradient basin floor. The 28 model runs in each model set consist of 2000 turbidity current flows at 1ky intervals, and include a constant sediment supply base case, then model runs with sediment supply oscillation amplitudes ranging from 50×10^7 m^3 to $150 \times 10^7 m^3$, and periods ranging from 20ky to 100ky, so a range from 20 turbidity flow events per oscillation to 100 flow events per oscillation (Fig. 2B). The changes in sediment input volume covers a range from small supply perturbations, to complete shut-down and then reactivation of the fan system (Fig. 2B) and represent a climate, tectonic or sea-level generated input signal produced by generation of turbidity currents on the slope or outer shelf

Comparison of the strata produced in the three model sets should indicate how a signal of varying amplitude and period is recorded in cases with no disruption from a simple, noise-free initial topography (Model Set 1), some disruption, similar to deposition onto some pre-existing but smooth depositional topography (Model Set 2) and maximum disruption, similar to deposition onto a very irregular previous depositional topography (Model Set 3). Comparison of individual runs within a set allows analysis of how signal strength is preserved for different amplitudes and periods.

2.3. Individual model parameters

Each individual model run has similar parameters to those used in Burgess et al. (2019) and consists of 2000 flow events at intervals of 1ky, therefore representing a duration of 2My. Flow event interval determines total calculated model duration, and the thickness of hemipelagic strata separating the resulting turbidite beds, but otherwise does not impact on model results because all analysis is carried out in thickness, not in time. Mean flow volume in all the runs is $1.0 \times 10^7 m^3$, producing a typical range of layer thicknesses from millimetres on the distal outer fan, to meters or even tens of meters in high-supply cases, in channels, and on the proximal inner fan.

2.4. Spectral analysis of the modelled strata

For each model run in each model set an average of around 13,000 vertical sections are analysed across the whole model grid, each with more than 50 greater-than-zero-thickness turbidite layers. Rigorous significance analysis determines if any statistically significant (i.e. very unlikely to occur by chance) periodicities are present in the succession. A power spectrum is calculated from each vertical section using a fast Fourier transform method. Statistical significance is determined using a non-parametric Monte Carlo approach in which a power spectrum is calculated for each of 250 realisations, each realisation being a randomly shuffled version of the beds in the vertical section (Burgess et al., 2019). When the power spectrum peak calculated from the original vertical section is absent in most of the randomly shuffled realisations, the spectral peak is demonstrated to be unlikely to occur in a chance arrangement of the strata, and therefore is considered to be statistically significant ($p<0.01$).

3. Results

3.1. Lobyte3D model behaviour

Despite a simple formulation, Lobyte3D displays emergent autogenic behaviour, such that flow routing evolves through time in a complex manner determined by the topography produced by prior history of deposition. All the Lobyte3D model runs show a channel cut into the slope from the fixed-position start point of each flow, and following the same course down the slope until around $y = 100$ km, after which lobe strata are deposited, forcing avulsions that cause divergence of channels and formation of further lobes along strike and further into the basin (Fig. 1A). Depositional lobes are groupings of around 50–150 flows that show compensational stacking (Fig. 2), and a generally retrogradational stacking pattern due to progressive backfilling of the feeder channel mouth, similar to the low Froude number examples in Wahab et al. (2022). In all these Lobyte3D runs, with or without an external signal, strata appear to be organised into packages that migrate both gradually

Table 1
Stratigraphic completeness values for all models in each set of models.

Model Set	Minimum simple stratigraphic completeness	Mean simple stratigraphic completeness	Maximum simple stratigraphic completeness
No noise	0.0005	0.0465	0.4345
Smooth noise	0.0005	0.0553	0.5109
Raw noise	0.0005	0.0735	0.5438

and suddenly through time (Fig. 2), show detectable thickening- and thinning-upward trends related to this migration (Burgess et al., 2019), and evidence of compensation stacking, all comparable with described lobate arrangements of deep-water fan strata (Van Dijk et al., 2009; Prelat et al., 2010; Wahab et al., 2022). Stratigraphic completeness is generally low, with mean values across each modelled fan of 5–7% measured as simple proportion of time recorded by turbidite deposition (Table 1).Note also that increased noise in the underlying topography does not reduce the stratigraphic completeness as might be intuitively expected; completeness in this case is mostly kept low by autogenic lobe switching, and disrupting that simple control with increased topographic noise tends to increase completeness because it produces intermittent deposition between the main lobes.

The described autogenic behaviour is all emergent in the sense that it is not directly or specifically prescribed in the model. For example, there is no rule in the model that directly says "deposit where previous deposition has not occurred". Instead this behaviour emerges from the basic flow routing and erosional and depositional physics represented in the model i.e. flow down-slope following the steepest-gradient available route, accelerating, decelerating and changing direction as the basin floor gradient dictates, with threshold velocities for erosion and deposition. This distinction is very important to distinguish this work from some analysis based on conceptual models where the conclusions are more directly defined by the input assumptions (e.g. Abels et al., 2013; Scotchman et al., 2015; Qi et al., 2022).

3.2. Spectral analysis of individual model runs

Spectral analysis of the strata from each model provides evidence for presence of statistically significant bed thickness trends in each vertical section across each model. Spectral analysis of all long-enough vertical sections from the constant sediment supply model from the "flat" initial topography model set shows that 99.7% of vertical sections analysed demonstrate strong evidence for non-random oscillations in bed thickness (e.g. Fig. 4C&D), while only around 0.3% of the analysed sections show no evidence for any non-random oscillations (e.g. Fig. 4A&B). An important point is that visual comparison alone does not allow distinction between strata with significant order (Fig 4C) and no significant order (Fig 4A).

A useful way to further analyse these power spectra from the modelled vertical sections is to calculate the total number of statistically significant ($p<0.01$) peaks at each period in the power spectra for all the vertical sections in each model (Fig. 5). Where an external signal is preserved, the count of significant peaks (blue lines, Fig. 5) should be higher than the count at the same period for the constant supply no-input-signal model (red lines) so that the difference β is positive, where

$$\beta = \sum_{x=f-\frac{1}{2}w}^{x=f+\frac{1}{2}w} \frac{C_{x\ (a>0)} - C_{x\ (a=0)}}{C_{x\ (a=0)}}$$

and C is the count of significant spectral peaks, a is amplitude of the supply oscillations, x is the period position in the series of the significant peak counts, f is the signal period, and w is the width of the window over which the signal magnitude is calculated. $C_{a>0}$ refers to period series of significant peaks counts for model runs with signal amplitudes greater than zero, and $C_{a=0}$ is the base-case significant peak count series.

The preserved signal strength β is definitely the case for higher-amplitude shorter-period input signals (e.g. periods 20ky and 30 ky, Figs. 5A, D and F), but less consistently the case for longer-period signals (e.g. periods 70ky and 100ky, Figs. 5C, F, and H) where there are higher number of significant peaks in the constant supply model baseline. This is demonstrating that autogenic processes create statistically significant non-random variations in bed thickness at longer periods, and in many cases these autogenic "signals" are as strong, or stronger in terms of number of significant peaks generated, than the variations produced by the external allogenic signal. This result suggests that identification of allogenic signals in deep-water strata may be more difficult than commonly recognised, and perhaps impractical in cases where a deep-water fan behaves as this model example behaves.

3.3. Spectral analysis of model sets

Three model sets have been run, each spanning a range of external sediment supply signal periods and amplitudes, and each with a particular initial topography with no noise content, smoothed random noise, or raw random noise. For each model run in each model set the number of significant power spectrum peaks within a periodicity window (the vertical pink bars in Fig. 5) was measured, converted to a normalised number of peaks per vertical section in the model, and plotted as a parameter space plot (Fig. 6) where the axes are the input signal period and amplitude and the colour coding indicates the preserved signal strength, green for a strong signal, red for weak or no allogenic signal (Fig. 6A, C, E). Parameter space plots show that strongest signals at the input period are preserved for longer-period input signals (e.g. Fig. 6A), and preserved signal strength decreases with increasing random noise in the model initial topography (compare Fig. 6A, C and E). Plotting β, the difference in significant peaks at the input signal period between each model run with an allogenic input signal varying sediment supply volume and the constant supply "base case" model run (Fig. 6B, D, and F) also demonstrates a significant point. Preserved significant signal magnitude β, in excess of the autogenic background, are more variable and sporadic compared to the number of peaks per vertical section plots (A, C, and E) with less systematic pattern of occurrence with period, except for consistently stronger preserved signal with greater input signal amplitude. The 20ky period highest-amplitude sediment supply oscillations produce a strong β signal in all three model sets, suggesting that shorter-period higher-frequency input signals are most likely to be preserved, even in the presence of other noise. The difference between e.g. Fig. 6A and B demonstrates that what appears to be an allogenic input signal is in fact mostly autogenic in origin because it is present, and often stronger, in the constant-supply base case model (Fig. 6).

Stratigraphic completeness in all the model runs is low, with mean values across all modelled fans ranging from 5 to 7% (Table 1). However, low mean stratigraphic completeness does not prevent spectral analysis from detecting autogenic and allogenic signals because only short fragments of any signal need be preserved to be detectable, and some sections have with completeness up to around 50% do occur (Table 1) and the analysis covers all vertical sections within the fan. Consequently, there is little-to-no relationship in these models between preserved signal strength and stratigraphic completeness (Fig. 7).

The spectral analysis (Fig. 6) includes all model layers, with many that are too thin to realistically manually observe and measure from outcrop (see layer thickness values in Fig. 4A and C). To test how these thin-bed data impact the analysis a similar analysis was run that excluded all layers less than 1 mm thick in all analysed vertical sections. Results are essentially similar (Fig. 8) showing the same tendency for stronger preserved input period signals for longer-period input signals (Fig. 8A, C and E) but also showing that much of this apparent allogenic signal is in fact autogenic in origin because it is present and often

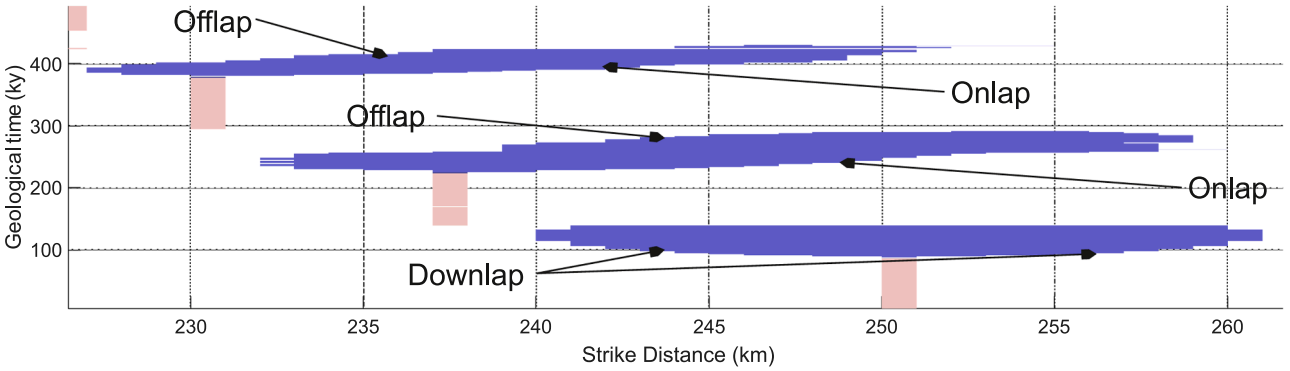

Fig. 3. A strike-oriented chronostratigraphic diagram showing three channel (pink) – lobe (blue) complexes developed during the first 500 ky of the constant supply no-noise model run (full chronostratigraphic diagram in Fig. 2A). Stratal terminations define a smooth downlapping stacking pattern symmetrical around the channel for the first lobe. Subsequent lobe stratal patterns are more complex, with combined onlap and offlap due to compensational stacking. For each lobe this autogenic stacking shows a consistent trend over 50–100 chrons, consistent with the periodicity determined by spectral analysis shown in subsequent Figs. 3-6.

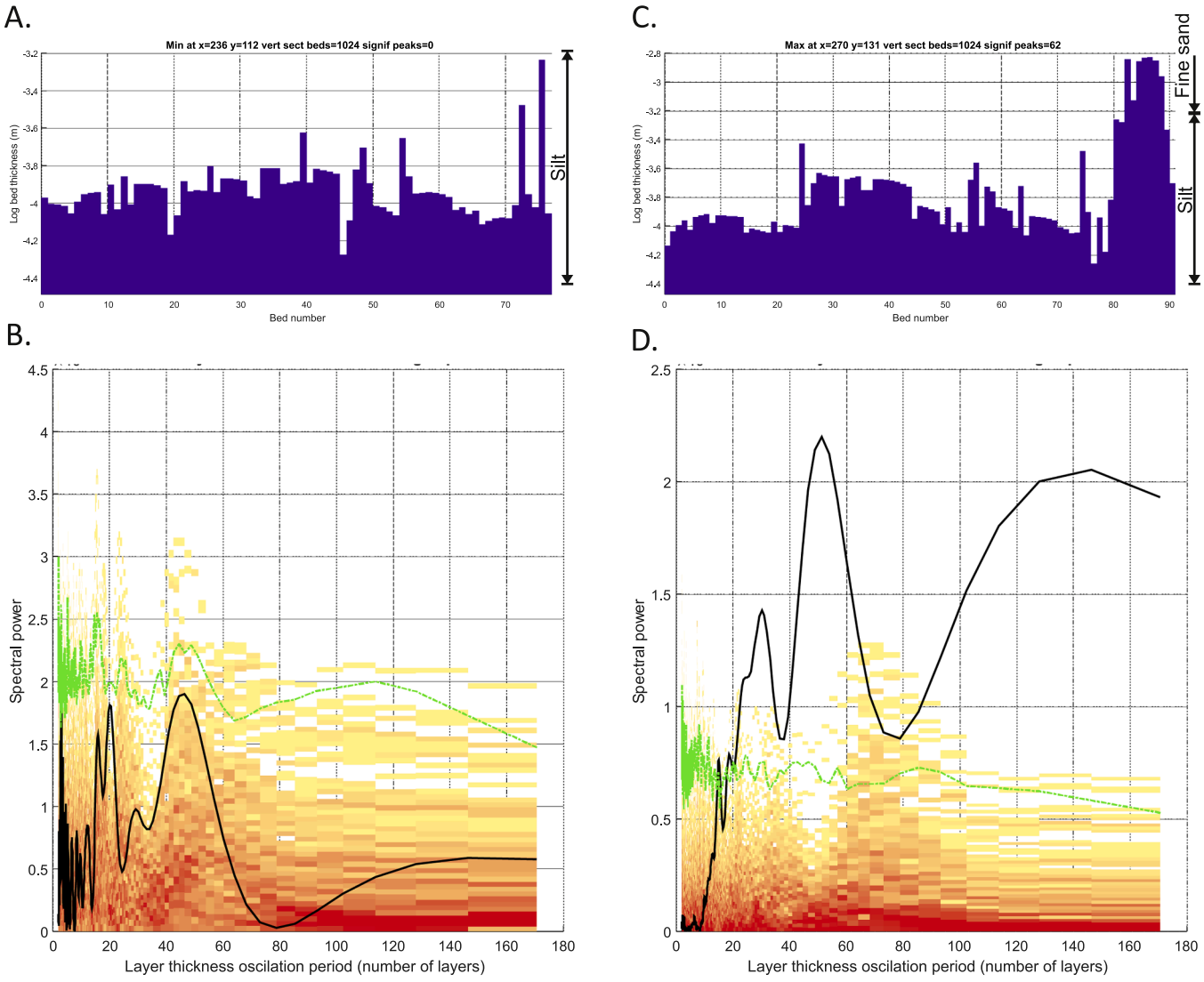

Fig. 4. From the no-noise topography constant supply model case a) Turbidite bed thicknesses from a vertical section at $x = 236$ km, $y = 112$ km B) Power spectrum (black line) from the same vertical section as A) which is all below the 99% significance level (green line) calculated from a Monte Carlo significance analysis (red-to-yellow rectangles, red is lower significance) indicating no significant peaks on the power spectrum c) Turbidite bed thicknesses from a vertical section at $x = 270$ km, $y = 131$ km D) Power spectrum from the same vertical section as C in the same format as B, with a power spectrum (black line) exceeding the 99% significance level (green line) for the maximum number of statistically significant points from this no-noise topography constant-supply case. Note that although very different in terms of level of autogenic signal present, the vertical section in C is not obviously more cyclical than A based on any visual analysis.

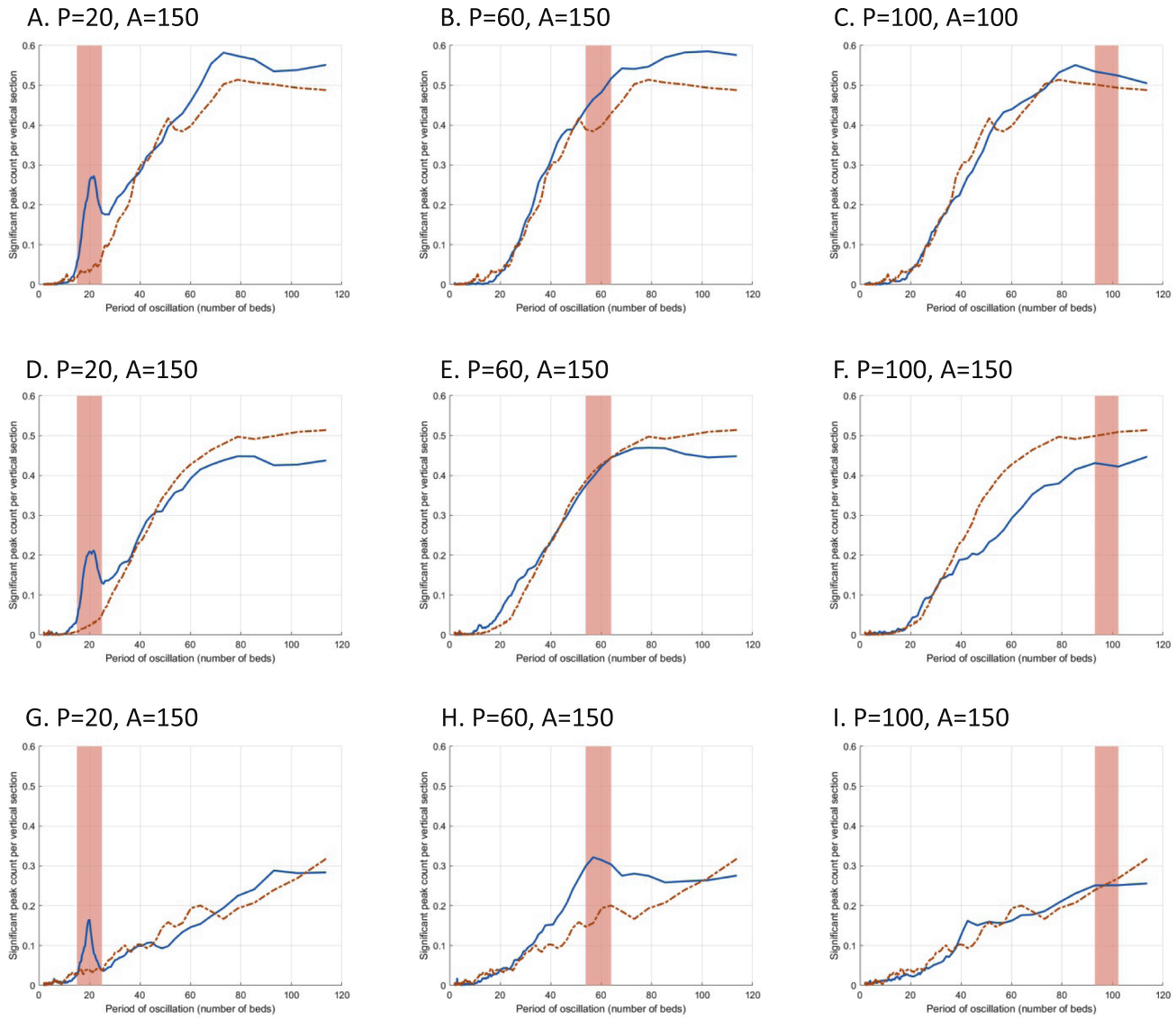

Fig. 5. Counts of the mean number of significant power spectra points (blue line) per vertical section, plotted against the period of oscillations present in the strata, both auto- and allogenic, for several model realisations with various periods (P) and amplitude (A) of supply oscillation input signals. In each plot the red dashed line is the equivalent count for the equivalent constant sediment supply case model, so with no external forcing signal meaning that all significant peaks recorded by the red line arise from autogenic processes. The pink band on each plot is centered on the x-axis around the input sediment supply oscillation signal period, and the width of the rectangle indicates the 3-point window over which the significant peak response is calculated. Examples A, B and C are from model cases with no-noise initial topography, D, E and F are from the model set with smooth noise topography, and G, H and I are from the model set with raw noise topography. Note how the high-frequency signal examples ($P = 20$ in A and D, $P = 30$ in F) have quite distinct bumps at the input signal period, but the situation is more variably complex with longer period input signals where the number of autogenic significant peaks on the power spectra is higher.

stronger in the constant supply base case model (Fig. 8B, D and F).

3.4. Autogenic cycle bundling

Cyclical strata composed of two or more periods with a five-to-one ratio are often taken as strong evidence for a preserved signal of orbital forcing because two key frequencies of orbital oscillations are calculated to have this ratio (Weedon, 2003; Abels et al., 2013; Waltham, 2015). However, analysis of the power spectra across each of the three constant-supply model realisations shows that 5:1 ratios are also common in these modelled autogenic cycles, covering 27–72% of the fan area (Fig. 9C, E and G) based on simple identification of all significant cycle periods with this ratio (Fig. 9A). Even a very conservative approach where only isolated power spectrum peaks are identified and compared (Fig. 9B) shows a few hundred sections in each modelled fan (1–2% of the total fan area) with the required 5:1 ratio (Fig. 9D, F and H). For the analysis identifying 5:1-ratio pairs in all significant points on the power spectra, the proportion of the fan area where bundling occurs decreases from 72% for the no random noise constant supply model, to 53% for the smoothed random noise, and 27% for the raw random noise model. This decrease shows how autogenic bundling can be disrupted by random noise in the depositional system.

4. Discussion

Burgess et al. (2019) showed that presence of an external signal in submarine fan strata could be indicated by presence of a "signal bump", identified via Fourier spectral analysis of bed thicknesses in vertical sections through fan strata. The signal bump is an excess of these statistically significant spectral peaks, relative to a base-case constant supply reference. Since there is no external signal in the base-case models, all the significant peaks in those base-case models must be

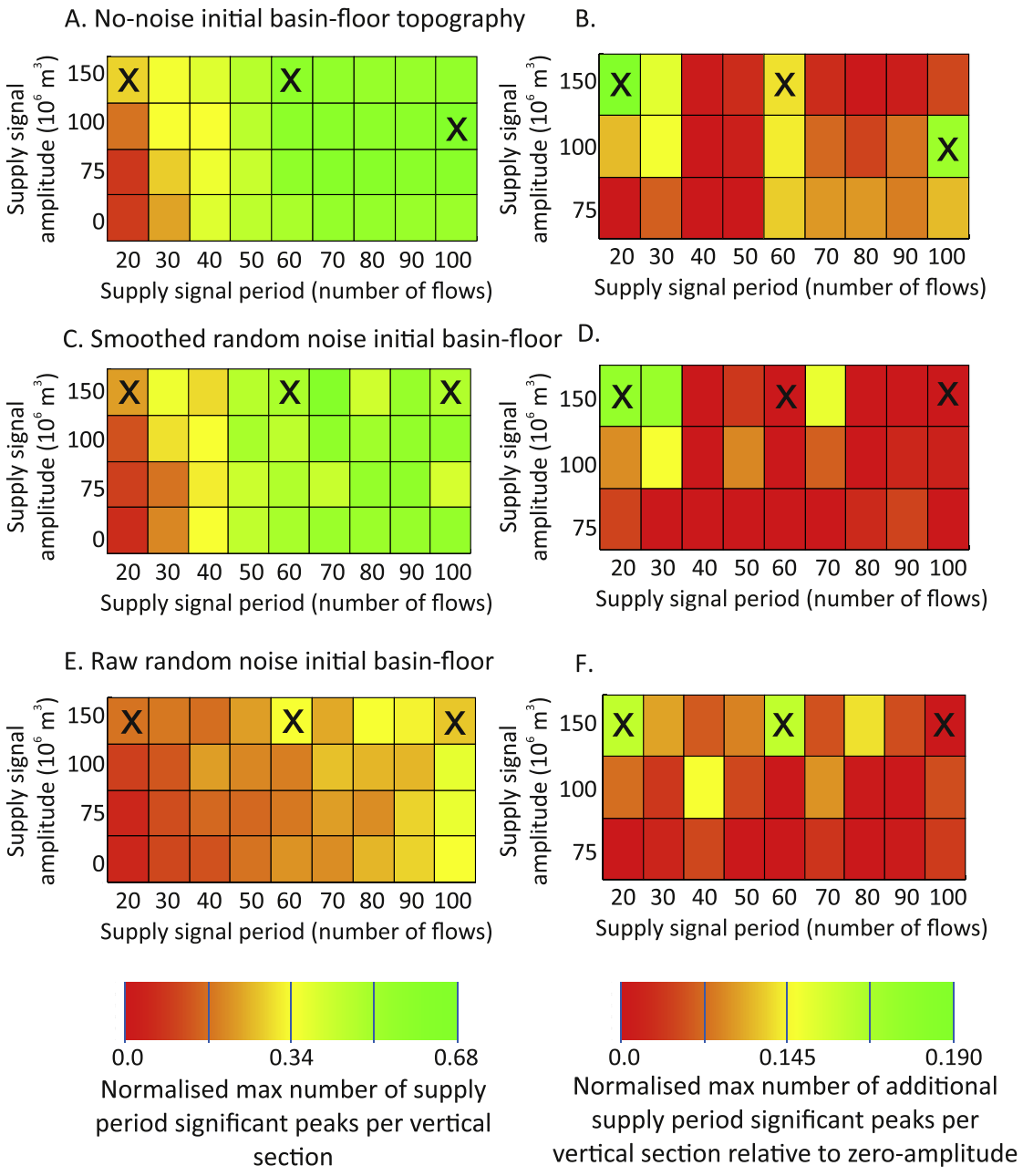

Fig. 6. A, C, and E. Parameter space plots of preserved signal magnitude. Each square represents one model run with supply oscillations of the amplitude and period specified by the axis values, and each grid is a different model set with either no-noise, smoothed-noise or raw-noise initial topography. Each square is colour coded to indicate the maximum number of significant spectral peaks per vertical section counted within a 10-bed period window of the input signal period (vertical pink stripes in Fig. 5), and normalised against the maximum number of significant peaks observed in one section in any of the analysed models. The colour is therefore a measure of the strength of input allogenic signal preserved in the model strata. Crosses in some grid boxes indicate the model examples shown in Fig. 5. Highest-magnitude signal indicators occur on the right of the parameter spaces, representing supply oscillation periodicities of 50ky and greater, and input signal preservation is most reduced in the raw random noise initial topography example. B, D and F. Parameter space plots of β, the number of significant power spectra peaks in excess of the number on the equivalent baseline constant supply model. The value of β is therefore a measure of the "signal bump", the allogenic signal present in each model run (see Burgess et al., 2019). Preserved significant signals in excess of the autogenic background in A, C and E are more variable and sporadic than that background, with no systematic pattern of occurrence with period, except for generally stronger preserved signal with greater input signal amplitude, and consistently best preservation of the shortest-period, high-frequency high-amplitude input signal (period 20 beds, amplitude 150 $\times$ $10^6 m^3$.

autogenic. This analysis extends this point to show how the signal bump is present or absent across a range of input signal periods, but most significantly these results demonstrate that, particularly for longer-period lower-frequency input signals, these may be entirely masked by autogenic periodicity in the strata. These autogenic periodicities arise from the basic stacking patterns developed in these modelled deep-marine fan data, for example due to avulsion, compensational stacking, and due to backstepping of lobe apexes up-dip as successive turbidity current flows interact with the depositional topography produced by previous flows (Fig. 2, Fig. 3). Similar autogenic effects on stacking patterns have been documented in analogue modelling of deep-water fan strata (Ferguson et al., 2020).

In contrast to the longer-period autogenic signal, the most consistently preserved allocyclic signals in this modelling are the highest-amplitude shorter-period highest-frequency 20ky signals. Preservation of only the higher-frequency allogenic signals is different from some

previous results indicating more likely preservation of lower-frequency signals (e.g. Toby et al., 2019; Griffin et al., 2023), because in these Lobyte3D models the autogenic effects are cyclical, not noisy, with a longer periodicity of 50ky and greater (e.g. Fig. 3). There are also some potentially important differences in the details of the analysis method e.g. 1D vertical sections versus a 3D volume analysis, but this requires further analysis to fully explore, particularly perhaps by expanding the analysis to multiple methods, not just spectral analysis. Specifically, many of the vertical sections are spatially correlated with other adjacent and nearby sections due to the same flows depositing across many vertical sections, so further analysis to understand the nature of this spatial correlation in two and three dimensions across the model will likely be useful.

The absolute periodicity values in this modelling are not significant since they stem from an essentially arbitrary choice of parameter value for the time interval between successive turbidity current flows and this does not impact on the model results beyond the thickness of interbedded hemipelagic strata, which is not analysed in the spectral analysis. However, the relative values of periodicity, so the difference between shorter-period dominant allogenic signals and longer-period dominant autogenic signals, may well be significant, reflecting the rates at which depositional topography develops, influences subsequent flow deposition and avulsion, and creates organised stacking patterns, as documented in other modelling and outcrop studies (e.g. Hawie et al., 2015; Li et al., 2020; Hajek & Straub, 2019). In these models that autogenic stacking is typically expressed at longer periods of 50–100 flows, so 50–100ky. More work can be done with Lobyte3D and other similar models to explore more fully exactly how and why these autogenic time scales develop, but we know that it is essentially controlled by the avulsion process, specifically the time required for channel backfilling to retrograde up the slope to the point sufficiently steep that a new flow has high enough velocity to divert around the previous flow and trigger an avulsion.

Also of particular significance in these model results is the decrease in both autogenic and allogenic preserved signal as the element of random noise present in the initial topography increases (compare Fig. 5G with 5A). Aside from the random noise component in two of the three model set initial conditions, there is no "stochastic sediment-transport dynamics ('noise')" (Straub et al., 2019) or "morphodynamic turbulence" (Jerolmack and Paola, 2010) in this modelled system, so the relationship between preserved signal magnitude and external forcing is a consequence of the influence of simple, deterministic autogenic processes, operating on particular timescales, shifting location of deposition through time, producing vertical sections of strata with a mean stratigraphic completeness of only 5–7% (Table 1).

As ever, it is important to consider the limitations of any numerical model being used to make interpretations and draw conclusions. For example, Straub et al. (2019) state that "many numerical formulations do not generate the rich structure of strata that is required to explore limits of environmental signal recovery because they do not account for the stochastic variability of processes that contribute to the construction of strata". The implication seems to be that only stochastic processes can generate the necessary variability to create realistic strata, but the strata produced by simple, deterministic Lobyte3D models suggest otherwise. The principle of parsimony advocates discovering the simplest model capable of producing an observed effect, as a proven method for understanding how dynamic systems work, and this is a strong argument for constructing the simplest possible reduced-complexity models that can explain observed stratigraphic features of interest. In this specific case, these numerical modelling results are useful because they suggest the minimum complexity required to mimic and mask an allogenic input signal with autogenic effects.

Another potentially important question to consider is whether failure to recover a longer-period allogenic signal is best explained as just a consequence of autogenic masking and the influence of random noise in the model topography, or if it should be considered indicative of the process often referred to as signal shredding? Paola (2017) stated that in shredding "the signal is not merely obscured but rather destroyed", and Straub et al. (2019) stated that "a signal that is shredded is not recoverable from stratigraphy regardless of the ability to date deposits, how wide the field of view is, or how many 1-D sections are averaged", both suggesting an important distinction between incompleteness and shredding. Jerolmack and Paola (2010) define shredding in a slightly different way as "the smearing of an input signal over a range of space and timescales by stochastic processes such that an input signal is not detectable at the outlet of a system". Importantly, the new results we present here further suggest that a signal bump analysis method can effectively reassemble a signal, even when only partially preserved in incomplete strata across several locations (Burgess et al., 2019). When this is not possible, and no signal is detectable by this method, for example in many models with a relatively strong random-noise component (Fig. 6e and F), it seems reasonable to consider this to be shredding as defined by Straub et al. (2020) because the signal is "not recoverable from stratigraphy regardless of the ability to date deposits, how wide the field of view is, or how many 1-D sections are averaged". Importantly, however, in these cases the lower-frequency signals are being effectively shredding by x inherent topographic noise and masked by autogenic processes, without the need for lots of erosion, or more complex dynamics. Further analysis is needed, with Lobyte3D and more complex numerical and analogue models, to explore how an autogenic threshold function (Toby et al., 2019) might be applicable in this case, particularly since the results presented here suggest preferential preservation of higher-frequency signals, not lower-frequency as suggested by Toby et al. (2022). Our new results also tend to support the view of Tofelde et al. (2021) that short frequency climate events may well be detectable in strata, depending very much on how the signal is defined, generated, transferred, and analysed, and whether autogenic processes are noisy or themselves periodic.

Finally, it is important to consider the implications of this analysis for identification and interpretation of Milankovitch frequency signals in strata, since this is a very common aim in analysis of this type applied to outcrop and subsurface strata. When analysing outcrop or core vertical sections, incidence of one or more statistically significant spectral peaks is typically taken to indicate allocyclic forcing of the strata, and the peak

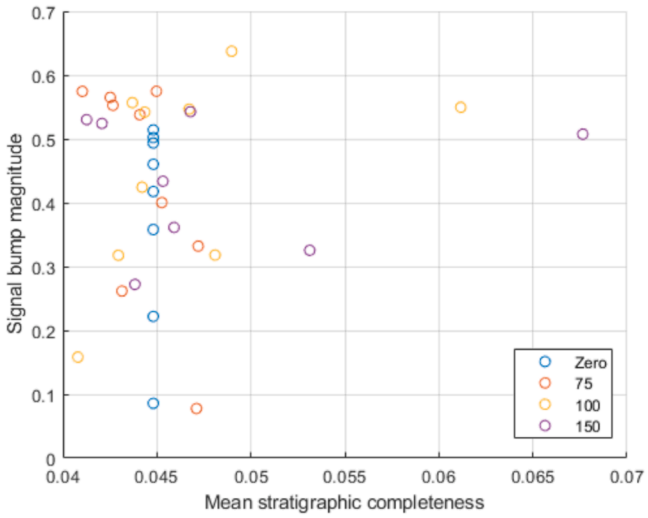

Fig. 7. B. Mean stratigraphic completeness across the submarine fan from all the models in the no-noise topography set, plotted against the magnitude of the signal recorded in each model. Scatter of data points and a lack of any significant linear trend indicates not relationship in these model results between stratigraphic completeness and signal preservation, most likely because the analysis covers all vertical sections within the fan, even short fragments of signal are detectable, and a few sections on each fan do have higher completeness, up to around 50% (Table 1).

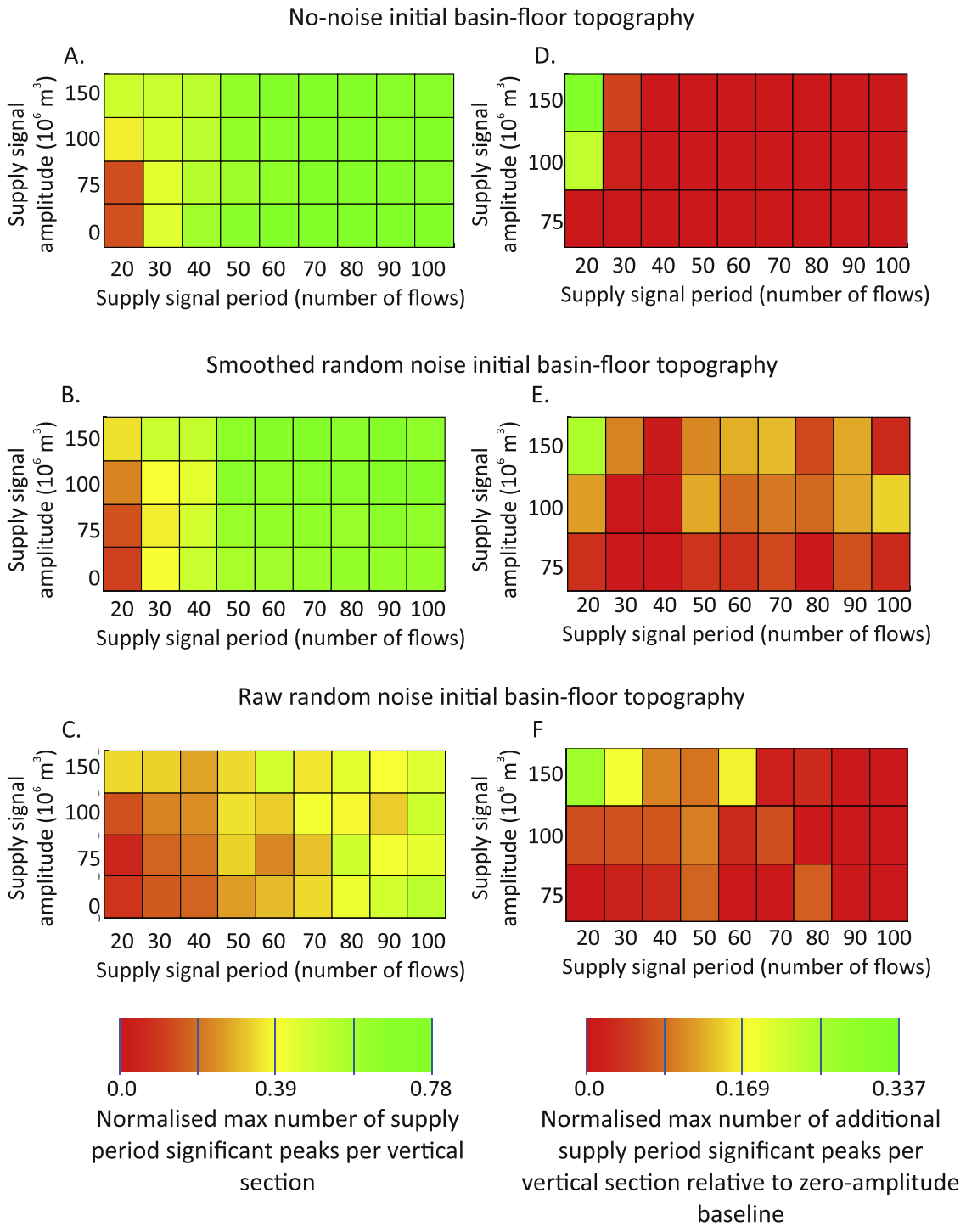

Fig. 8. Parameter space plots, in the same format as Fig. 6, but determined using power spectra calculated excluding any layers thinner than 1 mm that would be impractical to observe and measure in outcrop. Average number of vertical sections analysed per model in this case is around 7500 compared to around 13,000 in Fig. 6. Results from this thicker-layer-only analysis are very similar to Fig. 6, suggesting the result is robust even excluding thin-layer information. Most importantly, preservation of the shortest-period, high-frequency high-amplitude input signal (period 20 beds, amplitude 150 $\times$ 10^6m^3) is still consistently better than lower-amplitude and longer-period input signals.

frequency is typically estimated, or even just assumed, to fall "in the Milankovitch band" (Abels et al., 2013; Sinnesael et al., 2021). However, the model results presented here make this interpretation substantially more uncertain; the results show how autocyclic processes may be able to produce strong periodic signals in the strata that dominate in the power spectrum analysis, and could easily be misinterpreted as an allocyclic signal, even perhaps an orbitally forced allocyclic signal, which would be the most extreme interpretation error. Occurrence of 5:1 bundling ratios in the modelled autocyclic strata (Fig. 9) further increase the uncertainty. If many sedimentary systems include a strong component of autogenic processes generating a strong autocyclic signal, and it is quite possible that they do (e.g. Budd et al., 2016; Xi and Burgess, 2022), then simply assuming that identified cyclicity is allogenic in origin could be a serious error, even when 5:1 bundling is present, and especially if it leads to assumptions of chronostratigraphic and time scale calibration that are incorrect. Adopting a more rigorous

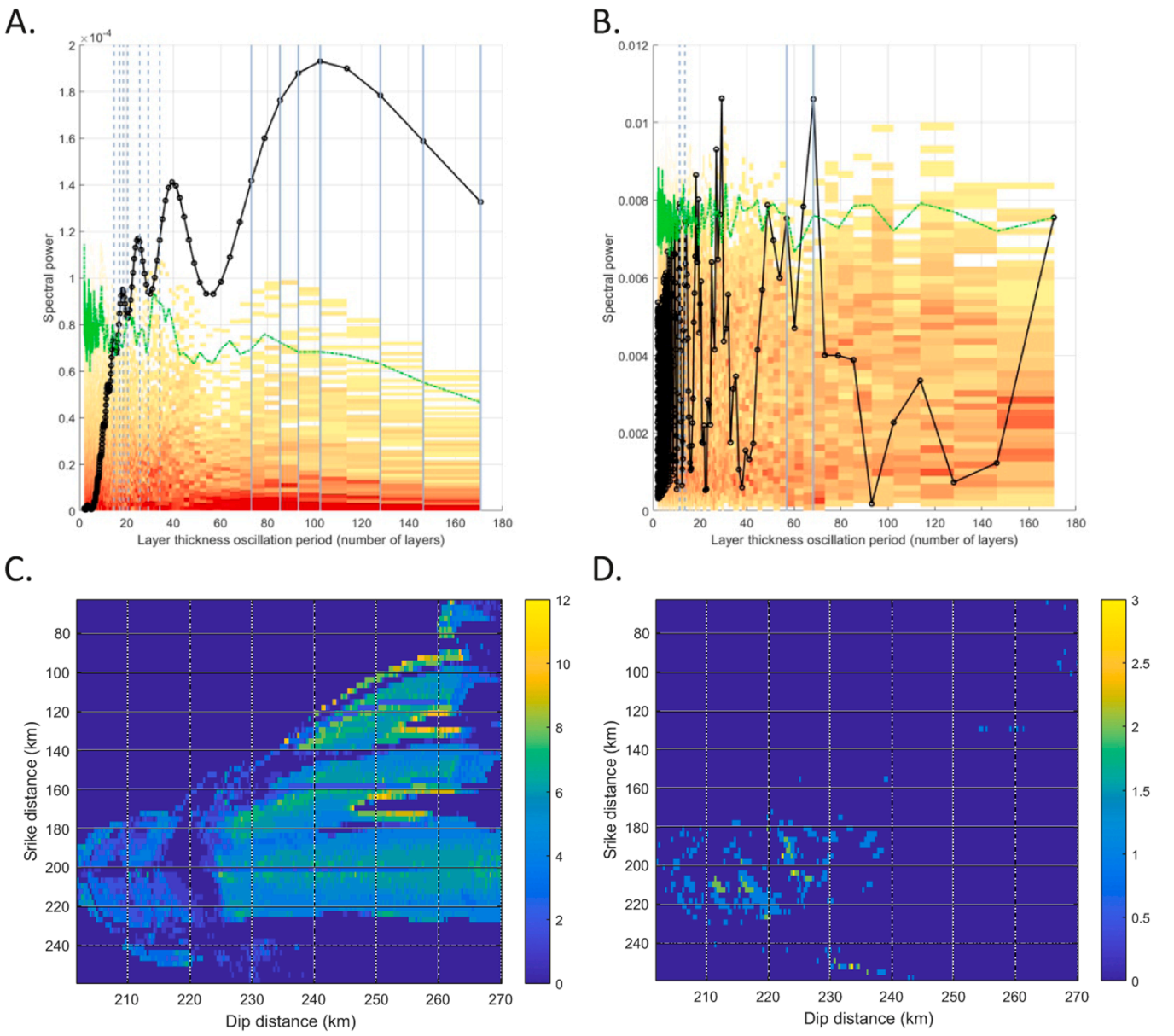

Fig. 9. A and B. Power spectra examples (black lines) showing periodicities that exceed a 99% significance level (green lines), determined via a non-parametric Monte Carlo randomised bed thickness calculation (red-to-yellow rectangles). Periods that show 5:1 ratios are marked by vertical solid and dashed lines, with a matching solid and dashed line for each bundle pair. In A bundles are identified from analysis of all significant points on the power spectrum, and in B only discrete peak periods within the significant powers are considered. C and D Maps of number of 5:1 bundles identified in the no-noise model for all peaks and discrete peaks respectively. E and F Maps of number of 5:1 bundles identified in the smoothed-noise model for all peaks and discrete peaks respectively. G and H Maps of number of 5:1 bundles identified in the raw-noise model for all peaks and discrete peaks respectively.

process of outcrop interpretation, for example using quantitative multiple hypotheses is probably sensible (e.g. Galloois et al., 2021), along with further work to determine if and how similar autogenic processes operate in more complex numerical and analogue forward models.

5. Conclusion

1. A reduced-complexity numerical forward model of down-slope sediment erosion, transport and dispersive deposition of submarine fan strata produces reasonably realistic strata that can be robustly analysed for signal content across model realisations with a range of external forcing amplitudes and periods.
2. Spectral analysis, including rigorous testing for statistical significance, shows that in most model runs autogenic dynamics dominate the cyclicity signal preserved in the strata, with the potential to mask even long-period, high-amplitude external signals. This autogenic cyclicity arises from lobe switching avulsions and smaller-scale flow-by-flow compensation effects combined with progradational and retrogradational stacking of the strata produced, for example, by progressive backfilling of channel mouths.
3. Spectral analysis shows that, using a constant supply no-external-signal model as an autogenic baseline, it is the highest-amplitude shortest-period allocyclic signal that is best preserved in the modelled fan strata. This occurs because in this case the autogenic lobe-forming processes are themselves strongly cyclical, with a similar period to the longer-period external signals, counter to many other analyses that tend to assume relatively high-frequency and noisy autogenic processes.

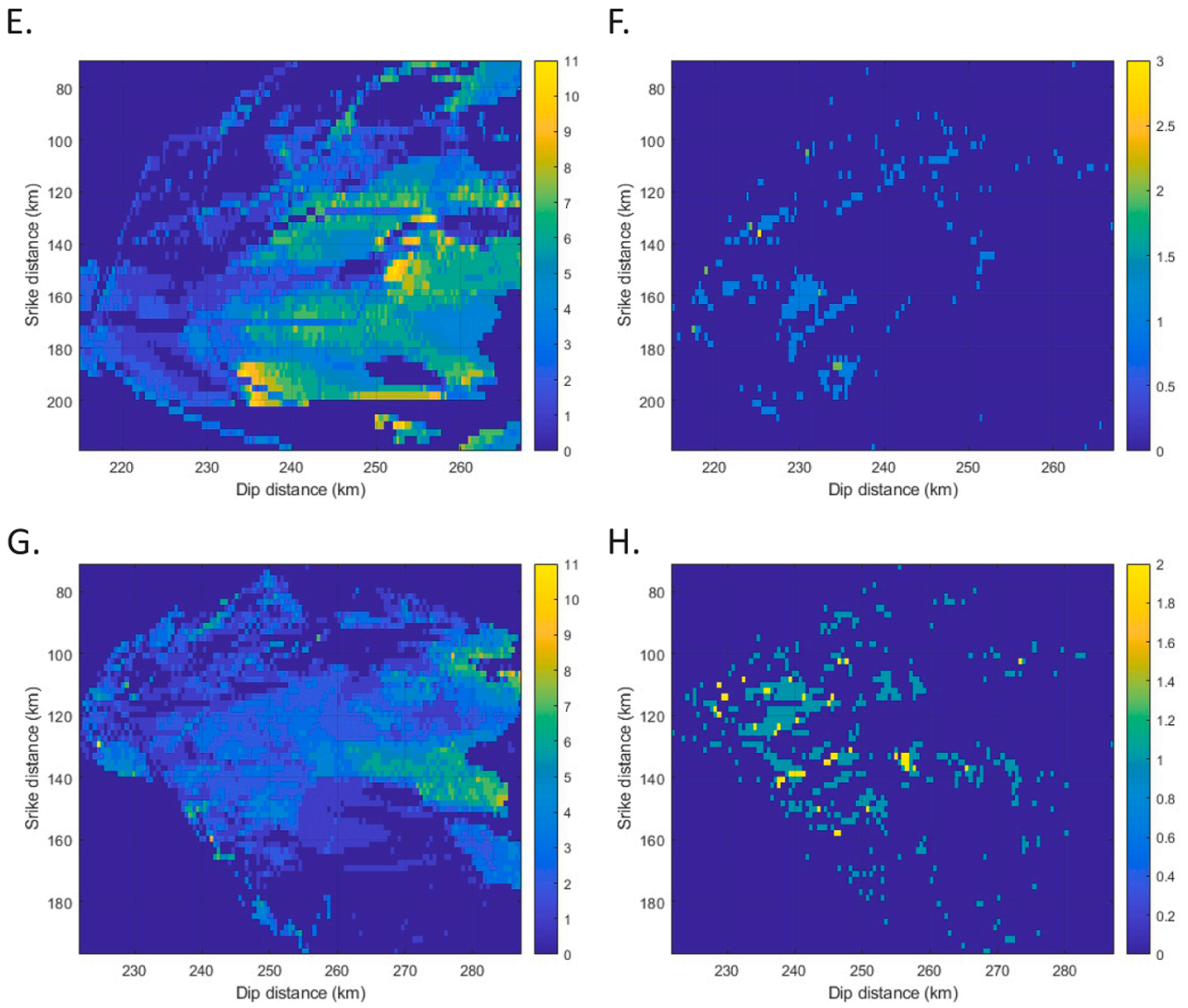

Fig. 9. (*continued*).

4. Spectral analysis also shows that the recorded and preserved signal recorded depends strongly on the level of noise present in the underlying topography; sea-floor topography with no noises preserves a stronger signal of external forcing than a topography with smoothed noise, which in turn preserves a stronger signal than the model runs on seafloor topography with raw, unsmoothed noise. This demonstrates how the complexity of the boundary conditions in the depositional system can determine signal strength even when the transport and depositional processes are themselves entirely deterministic.
5. This analysis suggests that we might be substantially underestimating the complexity involved in extracting a signal of external forcing from any strata where autogenic processes operate. The two different effects may often be practically indistinguishable, even using evidence such as 5:1 cycle bundling ratios, raising questions about the level of certainty required to justify use in chronostratigraphic time scales. Best-practice to address this uncertainty is perhaps a quantitative multiple-hypothesis approach (e.g. Gallois et al., 2021).

CRediT authorship contribution statement

Peter M. Burgess: Writing – review & editing, Writing – original draft, Visualization, Software, Methodology, Investigation, Formal analysis, Conceptualization. **Robert A. Duller:** Writing – review & editing.

Declaration of competing interest

The authors declare that they have no known competing financial interests or personal relationships that could have appeared to influence the work reported in this paper.

Data availability

Data will be made available on request.

Acknowledgements

Chris Stevenson, Alfie Mackie, Bingyi Chen and Ibrahim Tahiru all

helped develop and test the version of Lobyte3D used in this analysis. Silvio de Angelis provided useful advice on elements of the spectral analysis. Reviewers. Aaron Bufe and Glenn R. Sharman are thanked for particularly useful reviews that enhanced various aspects of the manuscript.

References

Abels, H.A., Kraus, M.J., Gingerich, P.D., 2013. Precession-scale cyclicity in the fluvial lower Eocene Willwood Formation of the Bighorn Basin, Wyoming (USA). Sedimentology 60, 1467–1483.

Allen, P.A., 2017. Sediment Routing systems: the Fate of Sediment from Source to Sink. Cambridge University Press, Cambridge, U.K., p. 407

Bernhardt, A., Schwanghart, W., Hebbeln, D., Stuut, J.B.W., Strecker, M.R., 2017. Immediate propagation of deglacial environmental change to deep-marine turbidite systems along the Chile convergent margin. Earth Planet Sci. Lett. 473, 190–204. https://doi.org/10.1016/j.epsl.2017.05.017.

Blum, M., Rogers, K., Gleason, J., Najman, Yani, Cruz, J., Fox, L., 2018. Allogenic and autogenic signals in the stratigraphic record of the deep-sea Bengal Fan. Sci. Rep. 8, 7973. https://doi.org/10.1038/s41598-018-25819-5.

Budd, D.A., Hajek, E.A., Purkis, S.J., 2016. Introduction to autogenic dynamics and self-organization in sedimentary systems. In: Budd, D.A., Hajek, E.A., Purkis, S.J (Eds.), Autogenic Dynamics and Self-Organization in Sedimentary Systems. SEPM Special Publication, pp. 1–4, 106.

Burgess, P.M., 2006. The signal and the noise: Forward modelling of allocyclic and autocyclic processes influencing peritidal carbonate stacking patterns. J. Sediment. Res. 76, 962–977.

Burgess, P.M., 2012. A brief review of developments in stratigraphic forward modelling, 2000–2009. In: Roberts, D.G. (Ed.), Regional Geology and Tectonics: Principles of Geologic Analysis. Elsevier, Amsterdam, pp. 379–404. https://doi.org/10.1016/B978-0-444-53042-4.00014-5.

Burgess, P.M., Masiero, I., Toby, S.C., Duller, R.A., 2019. A big fan of signals? Exploring autogenic and allogenic process and product in a numerical stratigraphic forward model of submarine-fan development. J. Sediment. Res. 89, 1–12. https://doi.org/10.2110/jsr.2019.3.

Chen, B., Burgess, P.M., Lin, C., Ren, L., Dong, C., Cao, Z., 2023. Extrinsic controls on turbidity fan lobes spatial distribution and potential reservoir presence prediction in half-graben lacustrine basin during early syn-rift: Insights from stratigraphic forward modelling. Mar. Pet. Geol. 155 https://doi.org/10.1016/j.marpetgeo.2023.106381.

Ferguson, R.A., Kane, I.A., Eggenhuisen, J.T., Pohl, F., Tilston, M., Spychala, Y.T., Brunt, R.L., 2020. Entangled external and internal controls on submarine fan evolution: an experimental perspective. The Depositional Record 6, 605–624. https://doi.org/10.1002/dep2.109.

Foreman, N.Z., Straub, K., 2017. Autogenic geomorphic processes determine the resolution and fidelity of terrestrial paleoclimate records. Sci. Adv. 3 e1700683 13.

Gallois, A., Burgess, P.M., Bosence, D., Hollis, C., 2021. Broken Beds, but better science; using multiple hypotheses to interpret geological data. Terra Nova 35, 73–82. https://doi.org/10.1111/ter.12631.

Granjeon, D., Csato, I., Catuneanu, O., 2014. Millennial-Scale Sequence Stratigraphy: Numerical Simulation with Dionisos. J. Sediment. Res. 84, 1–13. https://doi.org/10.2110/jsr.2014.36.

Griffin, C., Duller, R.A., Straub, K.M., 2023. The degradation and detection of environmental signals in sediment transport systems. Sci. Adv. 9. https://doi.org/10.1126/sciadv.adi8046.

Hajek, E.A., Straub, K.M., 2017. Autogenic Sedimentation in Clastic Stratigraphy. Annu. Rev. Earth Planet. Sci. 45. https://DOI:10.1146/annurev-earth-063016-015935.

Halsey, T.C., 2018. Erosion of unconsolidated beds by turbidity currents. Physics Review Fluids 3. https://doi.org/10.1103/PhysRevFluids.3.104303.

Harris, A.D., Covault, J.A., Madof, A.S., Sun, T., Sylvester, Z., Granjeon, D, 2016. Three-Dimensional Numerical Modeling of Eustatic Control On Continental-Margin Sand Distribution. J. Sediment. Res. 86, 1434–1443.

Hawie, N., Deschamps, R., Granjeon, D., Nader, F.H., Gorini, C., Muller, C., Montadert, L., Baudin, F., 2015. Multi-scale constraints of sediment source to sink systems in frontier basins: a forward stratigraphic modelling case study of the Levant region. Basin Research 29. https://DOI:10.1111/bre.12156.

Jerolmack, D.J., Paola, C., 2010. Shredding of environmental signals by sediment transport. Geophys. Res. Lett. https://doi.org/10.1029/2010GL044638.

Jobe, Z.R., Sylvester, Z., Parker, A.O., Howes, N., Slowey, N., Pirmez, C., 2015. Rapid adjustment of submarine channel architecture to changes in sediment supply. J. Sediment. Res. 85, 729–753. https://doi.org/10.2110/jsr.2015.30.

McNab, F., Schildgen, T.F., Turowski, J.M., Wickert, A.D., 2023. Diverse Responses of Alluvial Rivers to Periodic Environmental Change: Geophysical Research Letters v. 50 (10) e2023GL103075.

Paola, C., Heller, P.L., Angevine, C.L., 1992. The large-scale dynamics of grain-size variation in alluvial basins, 1: Theory: Basin Research 4 (2), 73–90 v.

Paola, C., Straub, K., Mohrig, D., Reinhardt, L., 2009. The "unreasonable effectiveness" of stratigraphic and geomorphic experiments. Earth Science Reviews 97, 1–43.

Paola, C., 2017. A mind of their own: recent advances in autogenic dynamics in rivers and deltas. In: Budd, D.A., Hajek, E.A., Purkis, S.J. (Eds.), Autogenic Dynamics in Sedimentary Systems: SEPM. Special Publication, pp. 5–17. https://doi.org/10.2110/sepmsp.106.04, 106.

Prelat, A., Covault, J.A., Hodgson, D.M., Fildani, A., Flint, S.S., 2010. Intrinsic controls on the range of volumes, morphologies, and dimensions of submarine lobes: Sedimentary. Geology 232, 66–76. https://doi.org/10.1016/j.sedgeo.2010.09.010 v.

Qi, K., Gong, C., Fauquembergue KellyFauquembergue, K., Zhou, Y., 2022. Did eustatic sea-level control deep-water systems at Milankovitch and My timescales?: An answer from Quaternary Pearl River margin. Sedimentary Geology. https://DOI:10.1016/j.sedgeo.2022.106217.

Scotchman, J.I., Pickering, K.T., Sutcliffe, C., Dakin, N., Armstrong, E., 2015. Milankovitch cyclicity within the middle Eocene deep-marine Guaso System, Ainsa Basin, Spanish Pyrenees. Earth Sci. Rev. 144, 107–121. https://doi.org/10.1016/j.earscirev.2015.01.007.

Sinnesael, M., McLaughlin, P.I., Desrochers, A., Mauviel, A., De Weirdt, J., Claeys, P., Vandenbroucke, T.R.A., 2021. Precession-driven climate cycles and time scale prior to the Hirnantian glacial maximum. Geology 49, 1295–1300. https://doi.org/10.1130/G49083.1.

Sharman, G.R., Szymanski, E., Hackworth, R.A., Kahn, A.C.M., Febo, L.A., Oefiner, J., Gregory, G.M., 2023. Carbon isotope chemostratigraphy, geochemistry, and biostratigraphy of the Paleocene–Eocene Thermal Maximum, deepwater Wilcox Group, Gulf of Mexico (USA). Climate of the Past 19, 1743–1775. https://doi.org/10.5194/cp-19-1743-2023.

Sheets, B.A., Hickson, T.A., Paola, C., 2002. Assembling the stratigraphic record: depositional patterns and time-scales in an experimental alluvial basin. Basin Res. 14, 287–301. https://DOI:10.1046/j.1365-2117.2002.00185.x.

Somme, T.O., Skogseid, J, Embry, P, Løseth, H, 2019. Manifestation of Tectonic and Climatic Perturbations in Deep-Time Stratigraphy – An Example From the Paleocene Succession Offshore Western Norway. Front. Earth Sci. (Lausanne) 20. https://doi.org/10.3389/feart.2019.00303.

Spychala, Y.T., Eggenhuisen, J.T., Tilston, M., Pohl, F., 2020. The influence of basin setting and turbidity current properties on the dimensions of submarine lobe elements. Sedimentology 67. https://doi.org/10.1111/sed.12751.

Straub, K.M., Duller, R.A., Foreman, B.Z., Hajek, E.A., 2019. Buffered, Incomplete, and Shredded: The Challenges of Reading an Imperfect Stratigraphic Record. J. Geophys. Res. Earth Surf. 125 https://doi.org/10.1029/2019JF005079.

Toby, S.C., Duller, R.A., De Angelis, S., Straub, K.M., 2019. A Stratigraphic Framework for the Preservation and Shredding of Environmental Signals. Geophys. Res. Lett. 46, 5837–5845. https://doi.org/10.1029/2019GL082555.

Toby, S.C., Duller, R.A., De Angelis, S., Straub, K.M., 2022. Morphodynamic limits to environmental signal propagation across landscapes and into strata. Nat. Commun. 13, 292. https://doi.org/10.1038/s41467-021-27776-6.

Tofelde, S., Bernhardt, A., Guerit, L., Romans, B.W., 2021. Times associated with source-to-sink propagation of environmental signals during landscape transience. Front. Earth Sci. 9, 628315 https://doi.org/10.3389/feart.2021.628315.

Vandekerkhove, E., Bertrand, S., Lanna, E.C., Reid, B., Pantoja, S., 2020. Modern sedimentary processes at the heads of Martínez Channel and Steffen Fjord, Chilean Patagonia. Marine Geology 419. https://doi.org/10.1016/j.margeo.2019.106076.

Van Dijk, M., Postma, G., Kleinhans, M.G., 2009. Autocyclic behaviour of fan deltas: an analogue experimental study. Sedimentology 56, 1569–1589. https://doi.org/10.1111/j.1365-3091.2008.01047.x.

Wahab, A., Hoyal, D.C., Shringarpure, M., Straub, K., 2022. A dimensionless framework for predicting submarine fan morphology. Nat. Commun. 13, 7563. https://doi.org/10.1038/s41467-022-34455-7.

Waltham, D., 2015. Milankovitch uncertainties and their impact on cyclostratigraphy. J. Sediment. Res. 85, 990–998. https://doi.org/10.2110/jsr.2015.66.

Weedon, G.P., 2003. Environmental cycles recorded stratigraphically. In: Weedon, G.P. (Ed.), Time-Series Analysis and Cyclostratigraphy: Examining Stratigraphic Records of Environmental Cycles. Cambridge University Press, pp. 161–216.

Xi, H., Burgess, P.M., 2022. The stratigraphic significance of self-organization: Exploring how autogenic processes can generate cyclical carbonate platform strata. Sedimentology 69, 1769–1788. https://DOI:10.1111/sed.12974.